sustainability

MDPI

Article

Calculation Method for Investigating the Behavior of Ground Surface Settlement of Underpass Buildings in TBM Double-Line Tunnels

Ting Ren [1], Hailong Zhang [2,*], Yuancheng Guo [1], Yang Tang [2], Qinglin Li [3] and Seisuke Okubo [4]

1 School of Civil Engineering, Chongqing Three Gorges University, Chongqing 404020, China
2 School of Civil Engineering, Chongqing University of Arts and Sciences, Chongqing 402160, China
3 School of Resources and Security, Chongqing University, Chongqing 400045, China
4 Department of Geo-System Engineering, The University of Tokyo, Tokyo 113-8656, Japan
* Correspondence: zhanghl@cqwu.edu.cn

Abstract: This study aims to investigate the behavior of ground surface settlement in TBM double-line tunnels constructed under existing buildings and to devise a calculative representation for that behavior. Numerical simulation and field monitoring methods were used to examine the Zhongcong Tunnel in Chongqing Metro Line 9. The ground surface settlement was analyzed using an orthogonal test of 3D numerical simulation methods. The results showed that ground surface settlement was influenced by TBM tunneling parameters and the location of the existing building in the following manner. The existing building reduced the settlement trough width. Surface settlement was increased by frictional and palm surface thrust forces but reduced by grouting pressure. The settlement trough width of the first excavation i_z correlated with that of the last excavation i_y. To accommodate the influence of existing buildings, the tilt factor of the settlement trough T_R was introduced to improve the formula for calculating the ground surface settlement of TBM double-line tunnels. The improved formula was validated by comparing the calculated results with actual measurements.

Keywords: TBM double-line tunnel; tunneling parameters; underpass existing buildings; ground surface settlement; calculation method; orthogonal experiments

Citation: Ren, T.; Zhang, H.; Guo, Y.; Tang, Y.; Li, Q.; Okubo, S. Calculation Method for Investigating the Behavior of Ground Surface Settlement of Underpass Buildings in TBM Double-Line Tunnels. *Sustainability* **2022**, *14*, 13410. https://doi.org/10.3390/su142013410

Academic Editors: Pengjiao Jia, Peixin Shi, Xi Jiang, Cheng Cheng and Jianjun Ma

Received: 21 August 2022
Accepted: 14 October 2022
Published: 18 October 2022

1. Introduction

Rapid urbanization has led to the need for and construction of more metro tunnels or underpasses. However, ground surface settlement caused by metro tunnel construction threatens the safety of existing buildings [1]. It is therefore necessary to investigate the effect of metro tunnel construction on ground surface settlement. The methods for studying ground surface settlement include field monitoring [2], empirical methods [3], and numerical simulations [4,5]. In actual tunnel projects, field monitoring methods are used. Since tunnel excavation causes strata disturbance, surface settlement is unavoidable; field monitoring can therefore provide timely analysis of the mechanism of surface settlement caused by tunnel excavation. Xu's [6] investigation using the field monitoring method led him to conclude that surface settlement is primarily caused by disturbances in the tunnel's surrounding rock during tunnel boring machine (TBM) excavation. The author also examined the influence of each surface settlement parameter. The research by Yu et al. [7] also showed that each phase of tunnel construction using TBM has a negative impact on surface settlement.

Even after obtaining the deformation parameters of the ground surface, it is still a challenge to predict the extent of ground settlement that will be caused by tunnel construction. Empirical methods are generally used to predict the actual effect of tunnel construction, with the seminal work of Peck [3] being a basis for other works in the tunnel construction industry. The ground settlement trough caused by tunnel construction follows the Gaussian law of normal distribution, and measured results show stratum loss to be the main cause of the ground settlement. Liu et al. [8], Han and Li [9], and Wei [10] reviewed the Peck formula because it was not adaptive to some local situations, reviewing the range of values and calculation methods for surface settlement parameters, and proposed a formula for calculating surface settlement in double-line tunnels using the superposition principle.

With developments in computer technology, numerical simulation methods have become an effective tool in the analysis of tunnel construction. Li et al. [11] investigated the mutual influence of the interactions between horizontal and inclined parallel tunnels using 3D numerical simulations. Wang et al. [12] introduced grouting pressure and palm surface thrust force in the finite element model to improve the accuracy of ground surface settlement calculations. Feng and Yu et al. [13] investigated the effects of the interaction of the left- and right-line tunnels on ground surface settlement using FLAC^{3D} and verified the effect of superposition on surface settlement in double-line tunnel excavations.

In the metro line plans of many cities, tunnels often have to underpass buildings and structures. This is because there is a space challenge for underground metro construction [14–17]. Liu et al. [18] provide a novel global sensitivity analysis method, namely the extended Fourier amplitude sensitivity test algorithm, to explore tunnel excavation-induced building disturbance. Dalgic et al. [19] used transfer functions to review the limiting tensile strain method, building response to tunneling, and excavation-induced ground movements. Lai et al. [20] used the finite difference method to study monitoring data and numerical simulations of the settlement characteristics of an existing tunnel. Xu et al. [21] studied tunneling-induced soil movements and deformation fields, framed building displacements, and structure shear distortions. However, few studies have investigated the effects of TBM tunneling parameters and existing buildings on surface settlement under composite strata conditions.

In this work, investigations were conducted on the Zhongcong Tunnel on Chongqing Metro Line 9. Using the numerical simulation orthogonal test, the influence of existing buildings on the settlement trough and the influence of TBM tunneling parameters on surface settlement were investigated. In addition, the formula for determining the surface settlement of double-line TBM tunnels was improved and applied to the Zhongcong Tunnel. The numerical simulation and calculation results were consistent with the actual measured results.

2. Project Description

Chongqing Metro Line 9 is a part of the Chongqing railway network, and the Zhongcong Double-line Tunnel is located in Chongqing Yubei District. The total lengths of the left and right lines are 1952.037 m and 1959.037 m, respectively. The underpass interval is 85.0 m long, and the overburden layer is 25.0 m. The geological structure of the surrounding rock is composite in nature, composed mainly of sandy mudstone, sandstone, and plain fill. The distance between the existing building and the right line is 7.5 m, the diameter of the tunnel is 6.6 m, and the distance between the left and right lines is 10.5 m. The location of the Zhongcong Tunnel and the horizontal plan of the investigation area are illustrated in Figure 1, while Figure 2 illustrates the cross section of the underpass and the existing building with its stratum profile.

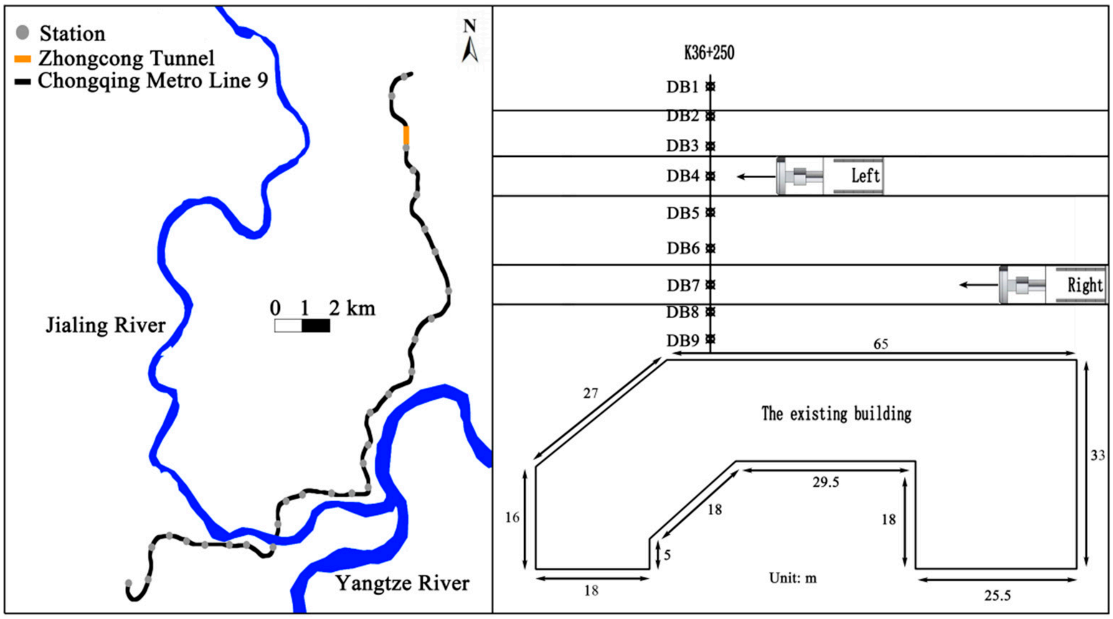

Figure 1. Location of Zhongcong Tunnel and horizontal plan of investigation area.

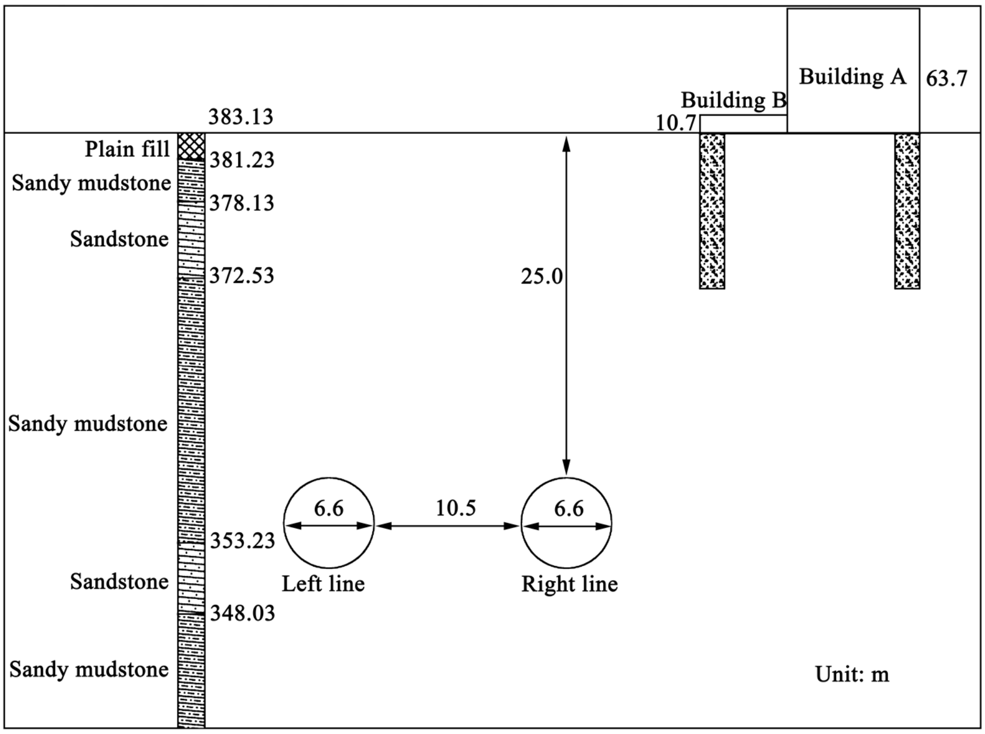

Figure 2. Cross-section of underpass location with strata profile for Zhongcong Tunnel.

3. Numerical Simulation

3.1. TBM Tunneling Parameters

Figure 3 illustrates the TBM tunneling parameters of the left and right lines in the underpass building; the total thrust ranges from 5500 to 11,200 kN in both lines, with an average approximately 8500 kN. The grouting pressure of the left line ranges from 0.18 to 0.30 MPa, while that of the right line ranges from 0.28 to 0.33 MPa. The average values of the grouting pressure in the left and right lines are approximately 0.25 MPa and 0.3 MPa, respectively.

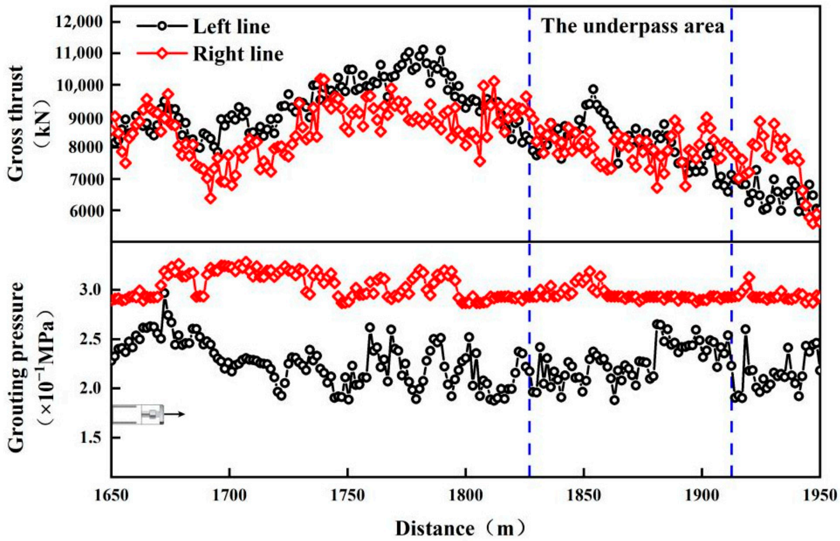

Figure 3. TBM tunneling parameters: Gross thrust and grouting pressure (Zhongcong Tunnel). The gross thrust is the thrust collected by the TBM sensor. The black and red lines represent the left and right tunnel lines, respectively.

The total thrust comprises the frictional force between the shield and the rock, the thrust force on the tunnel face, and other resistance. Guan [22] showed that other resistance is typically 1% to 5% of the total thrust. Therefore, the total thrust can be expressed as Equation (1):

$$F = F_N - F_f \tag{1}$$

where F_N is the thrust force on the tunnel face and F_f is the frictional force. Shi et al. [23] showed that the frictional force is smallest at the top of the tunnel and largest at the bottom. Therefore, F_f can be expressed as Equation (2):

$$\begin{aligned} F_f &= f_s + f_x \\ &= \tfrac{1}{2}\mu P_e \cdot S_c + \tfrac{1}{2}\mu(P_e + P_G) \cdot S_c \\ &= \tfrac{1}{2}\mu(2P_e + P_G) \cdot S_c \end{aligned} \tag{2}$$

where f_s and f_x are the frictional forces between the upper and lower parts of the shield, respectively; μ is the frictional factor, ranging from 0.1 to 0.3; P_e is the stratum pressure at the upper part of the shield; P_G is the strength of the reaction force produced by the shield self-weight on the shell; and S_c is the shield shell surface area.

3.2. Calculation Models

In the Zhongcong Tunnel project, the tunnel-boring machine dug 1.5 m with each move, and the excavation of the right line began after the left line was completed. Therefore, the simulation of the underpass construction included 180 moves. The simulation of the left line excavation comprised moves 1 to 90, while the right line simulation comprised moves 91 to 180, with the tunnel model length taken to be 135 m. The width and height were set as 120 and 58 m, respectively, to reduce the influence of boundary effects on the results. The roof of the tunnel was assumed to be the ground level, while the bottom of the tunnel was estimated to be four times the excavating diameter. Horizontal and vertical movements were restrained at the bottom of the model, but vertical displacements were freely distributed at the sides of the tunnel and at the ground surface. Figure 4 illustrates the dimensions of the model.

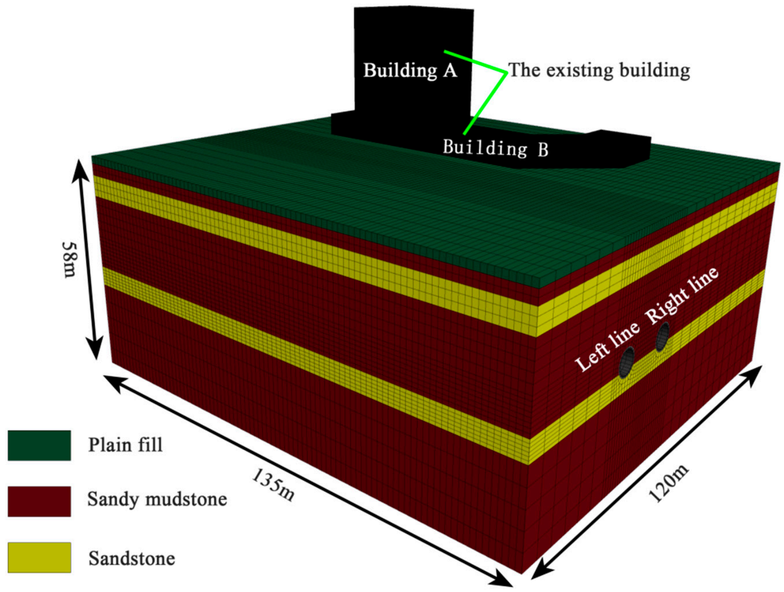

Figure 4. Dimensions of the model.

The numerical simulation was analyzed with FLAC^{3D} software, and the strata in the model were assumed to behave according to the Mohr–Coulomb theory. The shield shell of the TBM, synchronous grout, and segment were regarded as elastic materials. The equivalent load substitution method was used to simulate two existing buildings: Buildings A and B have 18 and 3 floors, respectively. The commuted load of each floor was taken to be 3 kN·m^2 [24]. The building pile was used as the pile structural unit in the software. Table 1 presents the parameters of the strata and materials.

Table 1. Parameters of strata and materials.

Properties	Plain Fill	Sandy Mudstone	Sandstone	Segment	Pile	Shield Shell	Grout in Soft Phase	Grout in Hard Phase
Volumetric weight γ (kN·m^{-3})	18	27.8	27.2	25	24	75.83	18	18
Elastic modulus E (MPa)	4.2	1620	4100	27,600	31,000	210,000	200	1800
Poisson's ratio υ	0.38	0.32	0.22	0.2	0.2	0.26	0.25	0.2
Cohesion c (kPa)	11	1720	7560					
Internal friction angle φ (°)	11	35	43.8					

To simulate the TBM dynamic construction process, the following parameters were considered: the influence of the palm surface thrust force, frictional force, grouting pressure, and gross thrust of the TBM tunneling parameters on the surface settlement. The stiffness transfer method was used to simulate the construction of the tunnel [25]. In the simulation, the average total thrust of the left and right lines was approximately 8500 kN. Equation (2) was used to calculate the frictional force F_f, which was approximately 4200 kN, with f_x and f_s being 1980 and 2220 kN, respectively. Equation (1) was used to calculate the palm surface thrust force F_N, which was 4300 kN. The average values of the grouting pressure in the left and right lines were approximately 0.25 and 0.3 MPa, respectively. Figure 5 illustrates the simulated excavation process.

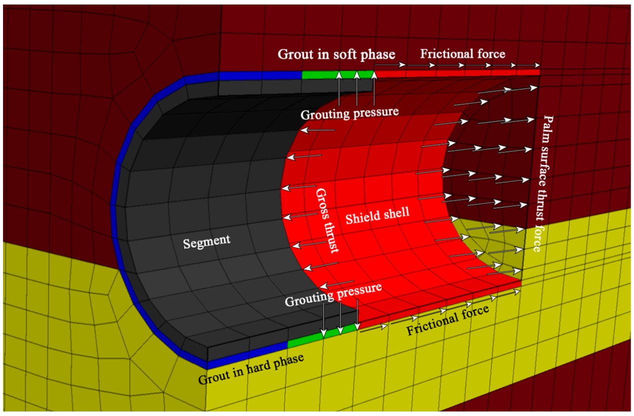

Figure 5. Simulation of the excavation process.

3.3. Model Validation

Figure 6 illustrates the ground surface settlement contours. The overburden stratum settlement was obviously affected by the existing building. The ground surface settlement was more severe in positions away from the underpass area than in the underpass area. Subsequently, the settlement trough width of the tunnel significantly increased in locations that were not contiguous to the existing building.

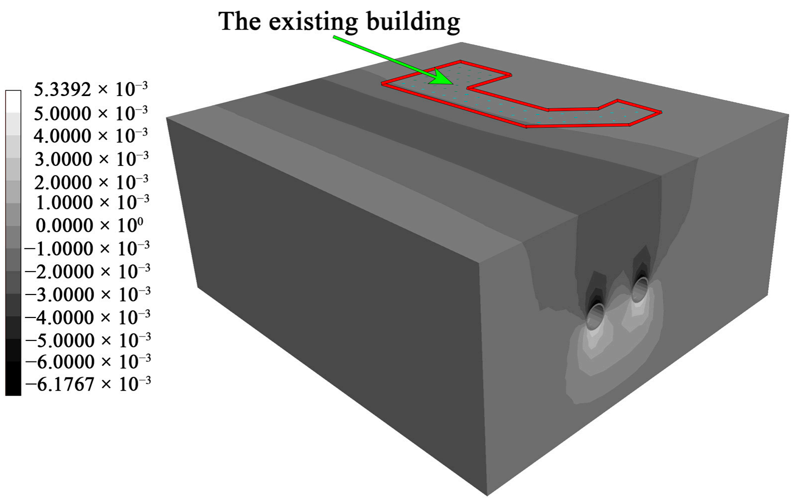

(**a**)

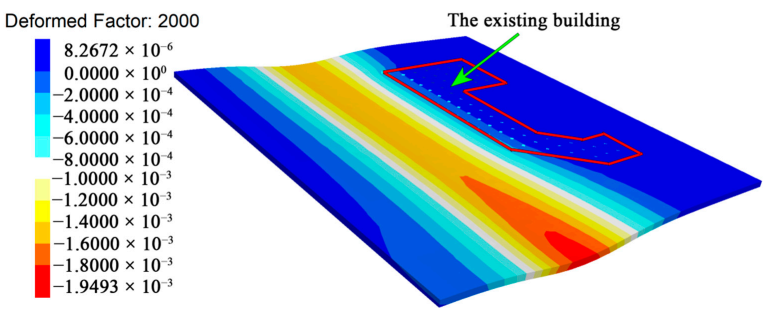

(**b**)

Figure 6. Settlement nephogram: (**a**) surrounding strata; (**b**) ground surface.

Figure 7 illustrates the calculated and actual measured results. The calculated results of the ground surface settlement were slightly lower than the actual measured results. The difference can be attributed to rock anisotropy: In the simulation model, the rock was assumed to have isotropic strata, which the actual rock may not have had. Thus, an unavoidable disparity is observable in the numerical simulation results. However, the settlement trends of the simulation and actual measured data were approximately the same. The consistency of the measured and simulated settlement results validates the accuracy of the model.

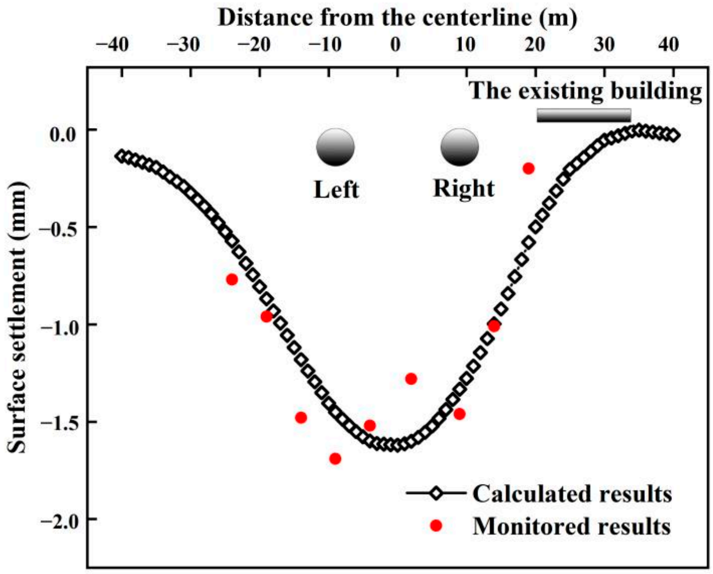

(**a**)

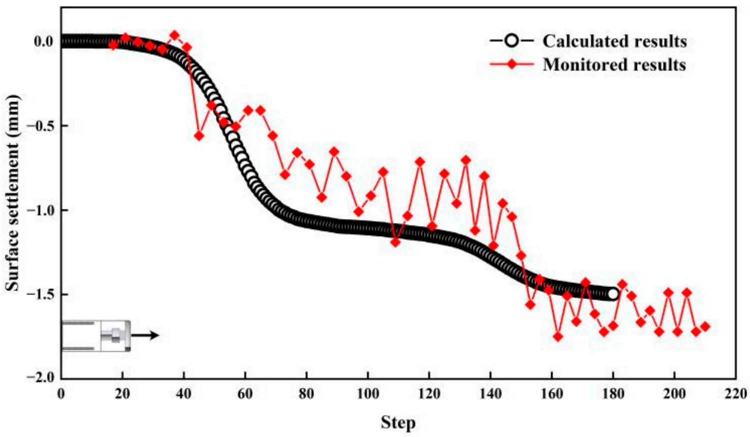

(**b**)

Figure 7. Numerical calculation and actual measured results: (**a**) Measured cross-section at K36+250; (**b**) DB4 monitoring point. The black and red lines represent calculated results and actual measured results, respectively (Zhongcong Tunnel).

4. Orthogonal Test

4.1. Orthogonal Experimental Design

The orthogonal experiment was designed as detailed in Table 2. In actual projects, the values of TBM tunneling parameters are dynamic; the grouting pressure and palm surface thrust force change with each move, and the friction factor μ constantly affects the friction force. Therefore, a permutation–combination scheme with three parameters at three levels and nine orthogonal numerical simulation schemes (L_9 (3^3)) was used to study the influence of the TBM tunneling parameters on ground surface settlement. The parameters are: grouting pressure (levels $1F_z$, $0.75F_z$, and $0.5F_z$), frictional force (levels μ = 0.1, 0.15, and 0.2), and palm surface thrust force (levels $1F_t$, $1.25F_t$,and $1.5F_t$). F_Z and F_t are the average values of grouting pressure and palm surface thrust force, respectively. The orthogonal experimental scheme for the numerical simulation is presented in Table 3.

Table 2. Influence factors and test levels.

Level	Grouting Pressure	Frictional Force	Palm Surface Thrust Force
1	$1F_z$	$\mu = 0.1$	$1F_t$
2	$0.75F_z$	$\mu = 0.15$	$1.25F_t$
3	$0.5F_z$	$\mu = 0.2$	$1.5F_t$

Table 3. Orthogonal experimental scheme for numerical simulation.

Number	Grouting Pressure	Frictional Force	Palm Surface Thrust Force
1	$1F_z$	$\mu = 0.1$	$1F_t$
2	$1F_z$	$\mu = 0.15$	$1.25F_t$
3	$1F_z$	$\mu = 0.2$	$1.5F_t$
4	$0.75F_z$	$\mu = 0.1$	$1.25F_t$
5	$0.75F_z$	$\mu = 0.15$	$1.5F_t$
6	$0.75F_z$	$\mu = 0.2$	$1F_t$
7	$0.5F_z$	$\mu = 0.1$	$1.5F_t$
8	$0.5F_z$	$\mu = 0.15$	$1F_t$
9	$0.5F_z$	$\mu = 0.2$	$1.25F_t$

4.2. Analysis of Experimental Results

The calculated results of the nine orthogonal test groups were determined, and the surface settlement that occurred after completing the double-line tunnel boring was analyzed, with measurements taken at the K36+250 Monitoring Section. The occurrences of ground surface settlement directly above the left- and right-line tunnels are expressed as S_z and S_y, respectively. The ground surface settlement that occurred directly above the centerline of the double-line tunnel is expressed as S_l. The orthogonal test results are presented in Table 4.

Table 4. Orthogonal test results above left-, center- and right-lines.

Number	S_z (mm)	S_l (mm)	S_y (mm)
1	−1.450	−1.620	−1.522
2	−1.626	−1.806	−1.698
3	−1.817	−2.009	−1.891
4	−1.553	−1.730	−1.627
5	−1.755	−1.943	−1.829
6	−1.732	−1.920	−1.809
7	−1.817	−2.009	−1.891
8	−1.716	−1.904	−1.794
9	−1.873	−2.070	−1.953

The averages of the different test levels and factors were calculated for S_z, S_l, and S_y; and expressed as $\overline{S}$. The extreme difference R was calculated, and the values of R were used to examine the degree of influence of each factor at each monitoring point [26]. Table 5 presents the calculated results.

Table 5. Influence of various factors on surface settlement.

Level	S_z (mm)			S_l (mm)			S_y (mm)		
	$\overline{S_{F_Z}}$	$\overline{S_{F_f}}$	$\overline{S_{F_t}}$	$\overline{S_{F_Z}}$	$\overline{S_{F_f}}$	$\overline{S_{F_t}}$	$\overline{S_{F_Z}}$	$\overline{S_{F_f}}$	$\overline{S_{F_t}}$
1	−1.631	−1.607	−1.633	−1.812	−1.786	−1.815	−1.704	−1.680	−1.708
2	−1.680	−1.699	−1.684	−1.864	−1.884	−1.869	−1.755	−1.774	−1.759
3	−1.802	−1.807	−1.796	−1.994	−2.000	−1.987	−1.879	−1.884	−1.870
R	0.171	0.200	0.163	0.182	0.232	0.172	0.175	0.204	0.162

Table 5 shows the degree of influence of each TBM tunneling parameter on surface settlement. The most significant impact comes from frictional force, followed by grouting pressure. The least impactful is palm surface thrust force. The values of $\overline{S}$ were analyzed for each factor but at different levels, and the following conclusions were drawn. Surface settlement increased as grouting pressure decreased. This is because reduced grouting pressure resulted in a reduction in the shield–tail void support pressure, thereby accelerating ground surface settlement. Increased frictional force resulted in a corresponding increase in surface settlement; as frictional force increased, the horizontal displacement of the surrounding rock increased, causing the shield-tail void to increase [27]. As the palm surface thrust increased, the surface settlement only increased gradually. These findings are consistent with the report by Xu [6]. The main reason for this phenomenon is that an increase in the palm surface thrust force resulted in an increase in the disturbance in the surrounding rock by the TBM.

5. Improved Ground Surface Settlement Equations

Peck, using a large dataset comprising measured engineering data, proposed Equation (3) for calculating lateral surface settlement, though his calculations involved only single-line tunnel excavations [3].

$$S(x) = S_{max}exp(-\frac{x^2}{2i^2}) = \frac{V_l}{i\sqrt{2\pi}}exp(-\frac{x^2}{2i^2}) \tag{3}$$

where $S(x)$ is the surface settlement at the horizontal coordinate, x, S_{max} is the surface settlement maximum value, V_l is the strata loss rate, and i is the settlement trough width.

Wei [28] derived a formula based on the Peck formula for calculating lateral surface settlement in double-line TBM tunnel excavations. The formula proposed by Wei [28] employs the superposition principle. To simulate ground surface settlement, the calculation can be expressed as Equation (4).

$$S(x) = S_{max\ z}exp\left[-\frac{(x+0.5l)^2}{2{i_z}^2}\right] + S_{max\ y}exp\left[-\frac{(x-0.5l)^2}{2{i_y}^2}\right] \tag{4}$$

where $S_{max\,z}$ and $S_{max\,y}$ are the maximum values of the surface settlement caused by the first and last tunnel excavations (i.e., the left-line tunnel and the right-line tunnel of the Zhongcong Tunnel), respectively; l is the distance between the left- and right-line tunnel axes; and i_z and i_y are the widths of the settlement trough caused by the first and last tunnel excavations, respectively.

Figure 8 illustrates the cross-section of the ground surface settlement of the nine test groups. As can be observed, the surface settlement affected the existing building, and all nine groups of the experimental settlement trough tilted toward the left tunnel line. Therefore, a tilt factor T_R was introduced into Equation (4). The improved formula can be expressed as Equation (5) below:

$$S(x) = T_R S_{max\ z}exp\left[-\frac{(x+0.5l)^2}{2{i_z}^2}\right] + S_{max\ y}exp\left[-\frac{(x-0.5l)^2}{2{i_y}^2}\right] \tag{5}$$

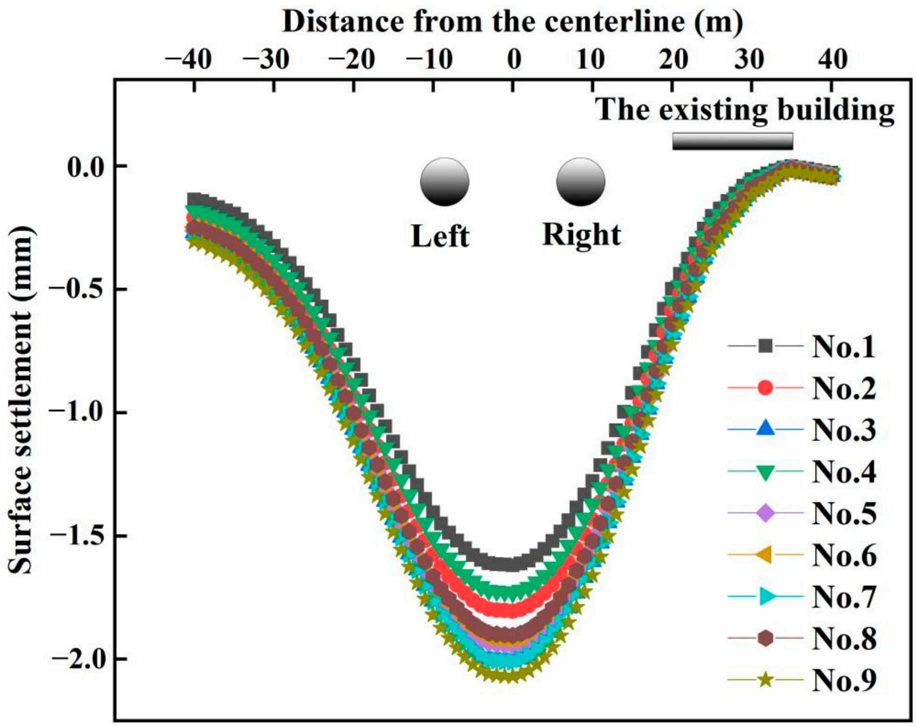

Figure 8. Cross-section of ground surface settlement at K36+250: Nos.1 to 9 are the calculated results of the nine orthogonal numerical simulation schemes presented in Table 3.

Table 6 presents the fitting analysis results of Equations (4) and (5). R^2 is greater in Equation (5) than in Equation (4); thus, the fit of Equation (5) is better. T_R has a smaller range (1.15–1.25), with an average of approximately 1.17. Therefore, this factor can reduce the error caused by the large range of the parameter values. The fitting results of i_z and i_y show that i_y increased as i_z increased, meaning i_z positively correlates with i_y. The fitting results of Equation (5) were plotted as shown in Figure 9, and i_z and i_y were fitted again.

Table 6. Fitting results of Equations (4) and (5) (K36+250). Settlements, widths and tilt factor. Coefficient of Determination is also shown.

Number	$S_{max\ z}$ (mm)	$S_{max\ z}$ (mm)	Equation (4)			Equation (5)			
			i_z (m)	i_y (m)	R^2	i_z (m)	i_y (m)	T_R	R^2
1	−1.106	−0.908	13.119	10.638	0.98664	12.384	9.362	1.151	0.99679
2	−1.216	−1.015	13.671	10.859	0.98208	12.883	9.426	1.161	0.99383
3	−1.344	−1.127	14.047	11.081	0.97981	13.265	9.584	1.160	0.99165
4	−1.168	−0.975	13.466	10.758	0.98351	12.688	9.370	1.160	0.99500
5	−1.296	−1.095	14.020	11.014	0.97848	13.206	9.474	1.167	0.99132
6	−1.287	−1.063	14.025	11.104	0.98169	13.254	9.632	1.157	0.99314
7	−1.255	−1.069	14.674	12.102	0.96924	13.553	9.770	1.243	0.99416
8	−1.266	−1.073	13.994	11.039	0.97913	13.182	9.508	1.167	0.99185
9	−1.369	−1.165	14.339	11.247	0.97688	13.538	9.665	1.165	0.98949

R^2 is 0.90665, as shown in Figure 9, which shows a good fit. Therefore, i_y can be expressed as Equation (6) below:

$$i_y = 0.291{i_z}^2 - 7.232i_z + 54.276 \tag{6}$$

As the distance between the left tunnel line and the existing building is large and less influenced by the existing building, the width of the settlement trough i_z above the left tunnel line can be calculated using Equation (7) a formula proposed by Wei [10] from fitting 22 data points of i.

$$i_z = m(r + h \cdot \tan\beta) \quad (7)$$

where m is the correction factor obtained from the fitting results presented in Table 6; with a range of 0.58–0.64, and an average of approximately 0.616; r is the tunnel radius, and h is the tunnel burial depth. $\beta = 45° - \varphi/2$, and φ is the weighted average of the internal friction angle of the strata in the upper part of the tunnel.

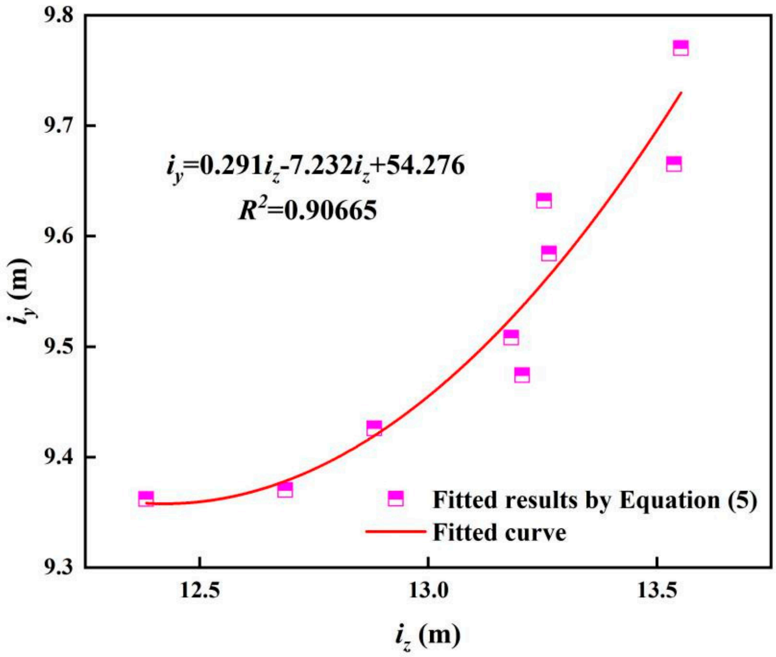

Figure 9. Correlations between i_z and i_y (the widths of the settlement by the first and last tunnel excavations).

6. Discussion

The average T_R and m (i.e., 1.17 and 0.616, respectively) were used to analyze the reliability of the improved surface settlement equation (i.e., Equation (5)). The values of i_z and i_y were calculated using Equations (6) and (7), respectively. $S_{max\,z}$ and $S_{max\,y}$ are the values of the surface settlement above the left- and right-line tunnel axes, caused by the excavation of the left and right lines, respectively. The calculated parameters are presented in Table 7.

Table 7. Calculated parameters.

$S_{max\,z}$ (mm)	$S_{max\,y}$ (mm)	T_R	i_z (m)	i_y (m)
−1.106	−0.908	1.17	13.112	9.480

Figure 10 illustrates the results of Equation (5) as well as the results of actual measurements taken at K36+250. The surface settlement curve obtained by Equation (5) is consistent with that obtained from the actual measured data. However, because of the range of values of m and T_R, the fitting equations for i_z and i_y are based on the Zhongcong Tunnel alone. Future research with a larger sample size would be required to test the validity of the equation parameters proposed.

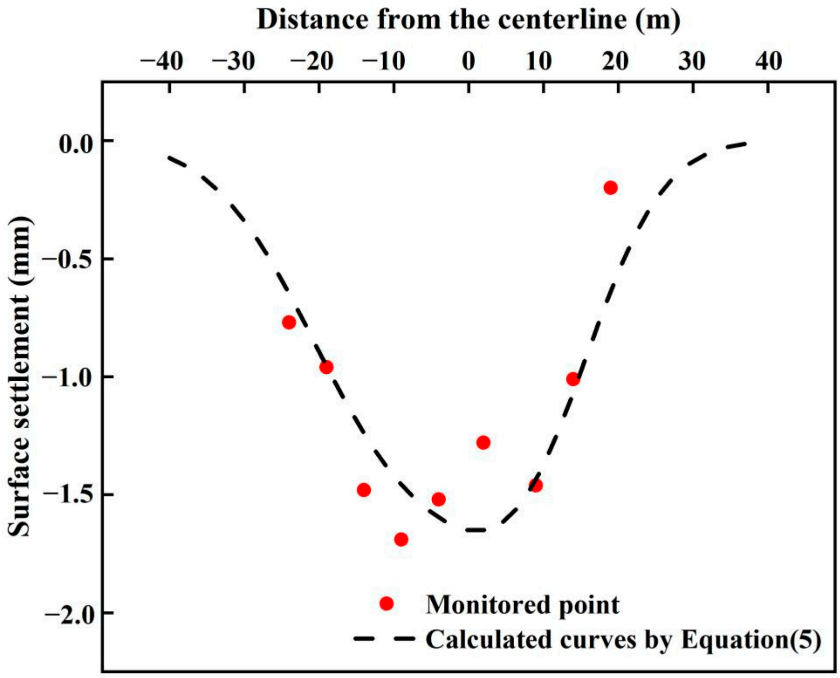

Figure 10. Actual measured and calculated ground surface settlement results. Red dots represent the actual measured results (Zhongcong Tunnel); black dashed line represents the calculated results of Equation (5).

7. Conclusions

The Zhongcong Tunnel was the research object of this study. Numerical simulation and field monitoring methods were used for investigating the effects of TBM parameters and existing buildings on ground surface settlement. An improved equation for calculating the ground surface settlement for TBM double-line tunnels was also proposed. The main conclusions of this work are summarized as follows:

(1) The location of existing buildings affects ground surface settlement. The ground surface settlement at the underpass area was less than that at the tunnel. The settlement trough width at the tunnel away from the existing building increased considerably.

(2) TBM tunneling parameters, grouting pressure, frictional force, and palm surface thrust force, exhibit varying degrees of influence on the ground surface settlement. The surface settlement increased as the frictional and palm surface thrust forces increased but decreased as grouting pressure increased.

(3) The formula for the surface settlement of the double-line TBM tunnels was improved by considering the influence of existing buildings; hence, the tilt factor of the settlement trough T_R was introduced. The settlement trough width of the first excavation i_z correlated with that of the last excavation i_y, the data of i_z and i_y were fitted, and the reliability of the improved equation was verified by comparing the actual measured results with the calculated results.

Author Contributions: Each author contributed to the paper. T.R., H.Z., Y.G., Y.T., Q.L. and S.O. conceived and designed the experiments. T.R. conducted the experiments and analyzed the experimental data. All authors have read and agreed to the published version of the manuscript.

Funding: This research was funded by the Natural Science Foundation of Chongqing, China (cstc2021jcyj-msxmX0354), the Key Project of Science and Technology of Chongqing Municipal Education Commission (KJZD-K202201304), the Scientific Innovation Project of Chongqing Graduate (CYS21491), the Open Fund for Master of Civil Engineering in Chongqing Three Gorges University (TMSL20TS08), and the Project of Major Cultivation in Chongqing University of Arts and Sciences (P2017JG18) for financial support.

Institutional Review Board Statement: Not applicable.

Informed Consent Statement: Not applicable.

Data Availability Statement: The data used to support the findings of this study are included within the article.

Conflicts of Interest: The authors declare that the research was conducted in the absence of any commercial or financial relationships that could be construed as a potential conflict of interest.

References

1. Comodromos, E.M.; Papadopoulou, M.C.; Konstantinidis, G.K. Numerical Assessment of Subsidence and Adjacent Building Movements Induced by TBM-EPB Tunneling. *J. Geotech. Geoenviron. Eng.* **2014**, *140*, 04014061. [CrossRef]
2. Fu, J.; Yang, J.; Zhang, X.; Klapperich, H.; Abbas, S.M. Response of the ground andadjacent buildings due to tunnelling in completely weathered graniticsoil. *Tunn. Undergr. Space Technol.* **2014**, *43*, 377–388. [CrossRef]
3. Peck, R. Deep excavations and tunnelling in soft ground. In Proceedings of the 7th International Conference on Soil Mechanics and Foundation Engineering, Mexico City, Mexico, 29 August 1969; pp. 226–290.
4. Gioda, G.; Swoboda, G. Developments and applications of the numerical analysis of tunnels in continuous media. *Int. J. Numer. Anal. Methods Geomech.* **1999**, *23*, 1393–1405. [CrossRef]
5. Liang, J.; Tang, X.; Wang, T.; Lin, W.; Yan, J.; Fu, C. Analysis for Ground Deformation Induced by Undercrossed Shield Tunnels at a Small Proximity Based on Equivalent Layer Method. *Sustainability* **2022**, *14*, 9972. [CrossRef]
6. Xu, Y.F. Analysis of ground surface settlement induced by shield construction. *Undergr. Eng. Tunn.* **2000**, *10*, 21–25. [CrossRef]
7. Yu, X.; Ren, H.; Hu, X. Analysis of the disturbance to surrounding soils during shield driving for the hangzhou metro line 1 project. *Mod. Tunn. Technol.* **2014**, *51*, 166–173. [CrossRef]
8. Liu, B.; Tao, L.G.; Ding, C.G. Prediction for ground subsidence induced by subway double tube tunneling. *J. China Univ. Min. Technol.* **2006**, *35*, 356–361. [CrossRef]
9. Han, X.; Li, N. Comparative analysis of strata prediction models for ground movement induced by tunnel construction. *Chin. J. Rock Mech. Eng.* **2007**, *26*, 594–600. [CrossRef]
10. Wei, G. Study on calculation for width parameter of surface settlement trough induced by shield tunnel. *Ind. Constr.* **2009**, *39*, 74–79. [CrossRef]
11. Li, X.; Du, S.; Zhang, D. Numerical simulation of the interaction between two parallel shield tunnels. In Proceedings of the CPTT 2012: Better Pipeline Infrastructure for a Better Life, Wuhan, China, 19–22 October 2012; pp. 1521–1533. [CrossRef]
12. Wang, F.; Miao, L.; Li, C. Numerical analysis of shield tunnel settlement considering construction process. *Chin. J. Rock Mech. Eng.* **2013**, *32*, 2907–2914. [CrossRef]
13. Feng, H.; Yu, R. Numerical analysis of influence of double—Line tunnel shield tunneling on ground surface settlement. *J. Railw. Eng. Soc.* **2019**, *36*, 78–83. [CrossRef]
14. Faherty, R.; Acikgoz, S.; Wong, E.K.; Hewitt, P.; Viggiani, G.M. Tunnel-soil-structure interaction mechanisms in a metallic arch bridge. *Tunn. Undergr. Space Technol.* **2022**, *123*, 104429. [CrossRef]
15. Franza, A.; Miraei, S.; Boldini, D.; Losacco, N. An equivalent beam approach for assessing tunnelling-induced distortions of frames with infills. *Tunn. Undergr. Space Technol.* **2022**, *129*, 104686. [CrossRef]
16. Klar, A. A Fourier-based elastic continuum solution for jointed pipeline response to tunneling. *Tunn. Undergr. Space Technol.* **2022**, *119*, 104237. [CrossRef]
17. Pirastehfar, K.; Shivaei, S.; Sadaghiani, M.H.; Nikooee, E. 3D numerical investigation of the effects of driving of the new mechanized tunnel on existing segmental linings and ground surface settlements-a case study: Shiraz metro line 2. *Int. J. Geotech. Eng.* **2022**, *16*, 878–889. [CrossRef]
18. Liu, W.; Wu, X.; Zhang, L.; Zheng, J.; Teng, J. Global sensitivity analysis of tunnel-induced building movements by a precise metamodel. *J. Comput. Civ. Eng.* **2017**, *31*, 04017037. [CrossRef]
19. Dalgic, K.D.; Hendriks, M.A.N.; Ilki, A. Building response to tunnelling-and excavation-induced ground movements: Using transfer functions to review the limiting tensile strain method. *Struct. Infrastruct. Eng.* **2018**, *14*, 766–779. [CrossRef]
20. Lai, H.; Zheng, H.; Chen, R.; Kang, Z.; Liu, Y. Settlement behaviors of existing tunnel caused by obliquely under-crossing shield tunneling in close proximity with small intersection angle. *Tunn. Undergr. Space Technol.* **2020**, *97*, 103258. [CrossRef]
21. Xu, J.; Franza, A.; Marshall, A.M.; Losacco, N.; Boldini, D. Tunnel–framed building interaction: Comparison between raft and separate footing foundations. *Géotechnique* **2021**, *71*, 631–644. [CrossRef]
22. Guan, H. Study on the Calculating Models of Key Parameters & Mechanical Behavior of the EPB Shield Machine. Ph.D. Thesis, Southwest Jiaotong University, Sichuan, China, 2008.
23. Shi, C.; Peng, L.; Lei, M. Study of time-space united calculating method of stratum deformation caused by shield tunnel excavation. *Rock Soil Mech.* **2009**, *30*, 2379–2384. [CrossRef]
24. He, M.D.; Liu, J.; Le, G.P.; Wang, M.; Zhang, D. Study of impact of shield tunneling side-crossing on adjacent high buildings. *Chin. J. Rock Mech. Eng.* **2010**, *29*, 603–608.
25. Lin, Z.J. *Study on Effect of Construction of Undercrossing Shield Tunnel on Existing High-Speed Railway Tunnel and Its Control Technology*; Central South University: Changsha, China, 2013.
26. Ren, L.Q. *Optimum Design and Analysis of Experiments*; Higher Education Press: Beijing, China, 2003; pp. 23–24.

27. Lai, H.P.; Wang, T.T.; Zhang, L.J.; Yuan, Y.; Luo, W. Construction control of shield tunneling underneath existing metro tunnel considering friction between shield shell and soil. *Tunn. Constr.* **2021**, *41*, 729. [CrossRef]
28. Wei, G. *Evaluation and Control of Environmental Effects of Double-Line Shield Tunnel Construction*; Architecture and Building Press: Beijing, China, 2018; pp. 56–60.